Morphological characterization of reaction injection moulded *(RIM)* polyester-based polyurethanes

Israel D. Fridman* and Edwin L. Thomas†
Polymer Science and Engineering Department, University of Massachusetts, Amherst, Massachusetts 01003, USA
Ly James Lee‡ and Christopher W. Macosko
Department of Chemical Engineering and Material Science, University of Minnesota, Minneapolis, Minnesota 55455, USA
(Received 9 August 1979; revised 20 November 1979)

Characterization studies of reaction injection moulded (*RIM*) processed (*in-situ* polymerized) polyester-based segmented thermoplastic polyurethane have been performed utilizing various morphological techniques. The fast and exothermic urethane polymerization results in large temperature gradients in the mould which influence molecular weight and morphological structures. The present work is conducted to draw relationships between sample morphology and the processing conditions utilized to form the polymer.

INTRODUCTION

The importance of phase separation in polyurethanes for the elucidation of structure–property relationships was first proposed by Cooper and Tobolsky[1] in 1966. Considerable efforts towards the understanding of the nature of phase separation[2–7], and the consequences for the bulk properties of the materials[8–10] have since been made. Several models of phase-segregated polyurethane systems[11–15] have been proposed. Previous work, however, has concentrated on polyurethanes which have been quiescent during approximately isothermal polymerization, starting from well mixed components. Little is known about the morphology of polymerizing mixtures subjected, for instance, to temperature gradients.

Reaction injection moulding, (*RIM*), is a relatively new polymer processing method which forms moulded parts directly from liquid monomers and oligomers by fast, *in situ* polymerization. A schematic diagram of the process is shown in *Figure 1*. A step-growth copolymerization of a polyol mixture containing either a polyester or polyether polyol and a low molecular weight diol with a diisocyanate takes place. The flow rates of the highly reactive components must be accurately controlled to provide the correct stoichiometry. Mixing is achieved by forcing the two metered streams to impinge on one another at high velocity. This operation is followed by rapid flow into the mould where polymerization proceeds. Commercial urethane polymerization can be very fast. Polymerization starts at the moment of impingement, proceeds in the runner and reaches a very high conversion in the mould with gel times typically less than 10 s. Finally, in as little as 1 min, the part may be ejected from the mould.

In urethane *RIM* polymerization, it is fundamental to understand how the process influences the structure and properties of the polymer formed. The polyurethane reaction is highly exothermic and *RIM* parts will develop a temperature profile due to the low thermal conductivity of the polymer in conjunction with substantial part thickness. Conversion and temperature profiles may bring about non-uniformities in molecular weight and segment distributions, domain formation, crystallinity, etc., which will subsequently influence physical properties.

For this study, a polycaprolactone diol/diphenylmethane diisocyanate/butanediol-based urethane was prepared, employing both high and low mould wall temperatures with relatively low catalyst concentration (gel time approximately

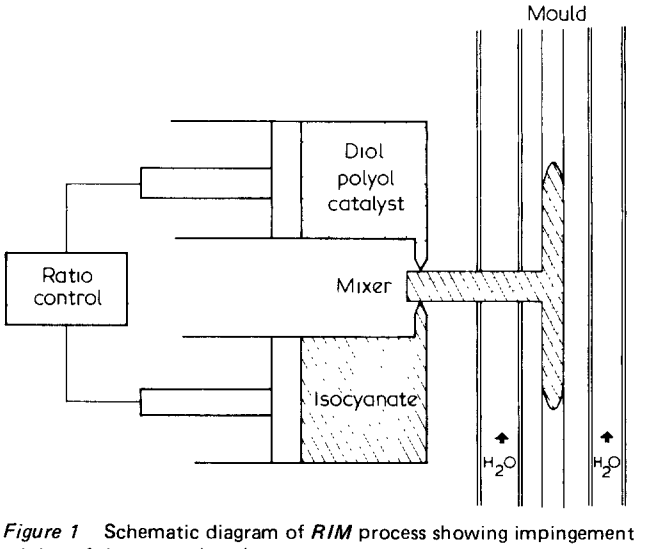

Figure 1 Schematic diagram of *RIM* process showing impingement mixing of the polyol/diol/catalyst and diisocyanate streams

* Present address: Polyvinyl Chemical Industries, Wilmington, Ma 01887, USA
† To whom correspondence should be addressed
‡ Present address: Research Division, The General Tire and Rubber Co., Akron, Ohio, USA

0032–3861/80/040393–10$02.00

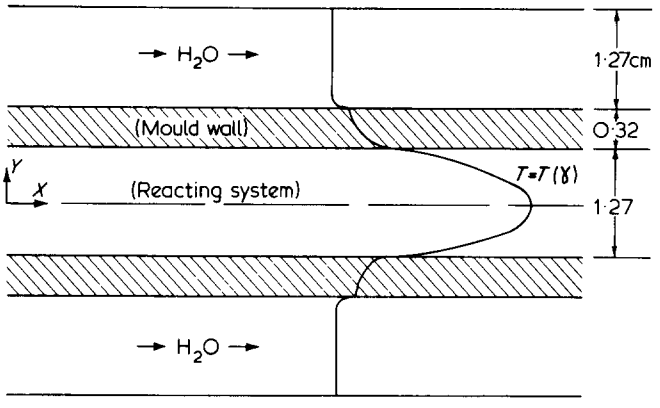

Figure 2 Schematic of *RIM* non-isothermal mould, showing assumed temperature profile

1 min). These 'slow *RIM*' samples permit a preliminary understanding of the structure variations as a function of mould temperature, providing better insight into the complex polymerization–phase separation–solidification–crystallization processes occurring during *RIM*.

EXPERIMENTAL

Chemical system

The polyurethane chosen for this study consists of a polyester soft segment based on a poly(ε-caprolactone diol) (PCP) (PCP-0200, Union Carbide Corporation) with a number-average molecular weight of 2000, and a hard segment based on 4,4′-diphenyl-methane diisocyanate (MDI) (Mondur M, Mobay Chemical Company) chain-extended with 1,4-butanediol (BDO) (Aldrich Chemical Company). Polymerization runs were carried out with a 1/6/5 mol ratio of PCP/MDI/BDO, corresponding to 43% wt of hard segment. Diol and BDO were used as received. Union Carbide reported a diol [OH] equivalent to 55.9 mg KOH/g diol, an acidity of 0.06% by wt and a water content of 0.01% by wt. MDI was purified by heating at 60°C for 2 h and filtering through a heated filter. Before reaction, the diol was melted and degassed at 65°C with a vacuum pump for at least 2 h until no further bubbles were evolved. The BDO was degassed at room temperature for ~20 min. The MDI was degassed at 60°C for 20 min after being filtered. The catalyst dibutyltin dilaurate (DBTDL-T12, M & T Chemicals) was used at a concentration 0.02 mol m^{-3}. All the reactions were at equivalent stoichiometry.

Polyurethane processing

Non-isothermal polymerizations were conducted in a water-heated *RIM* mould (see *Figure 2*) with the reactants at a temperature of 60°C. Two different mould temperatures were used, 85° and 37°C, designated as N1 and N2, respectively. The *RIM* mould consists of two aluminium plates (5/16 in. thick) 1/2 in. apart, which are cored for water cooling/heating. Centreline and mould wall temperature were recorded using thermocouples. The measured temperature profiles for both samples are shown in *Figure 3*. Reaction has begun before the reactants enter the mould, since the initial mould centreline temperature is already 80°C. The centreline temperature reaches a maximum of 170°C after 100 s for N1 and 152°C after 90 s for N2. Samples were termed N1-C or N1-S indicating that the sample was taken from the centre or surface of the mould. The gel time under adiabatic conditions for both samples is approximately 1 min. The N1 and N2 polymers were examined as processed without post-cure treatments. For comparison, samples were also prepared under isothermal conditions, at 70°, 90° and 110°C[23]. No catalyst was used in these reactions, to slow down the rate of polymerization and enable temperature control of the reacting mixture.

Transmission electron microscopy (TEM)

A SORVALL-MT2B ultramicrotome with a cryosection attachement was used to obtain suitable sections (of the order of 1000 Å thick) of the centre and surface of the polymers. Sections were obtained using glass knives with 45 degree cutting angle and propanol at −90°C as the liquid for floating sections. Sections were mounted on 400 mesh copper grids and allowed to dry overnight at room temperature. Bright field *TEM* micrographs of the specimens were obtained using a JEOL–100CX–TEMSCAN electron microscope operated at 100 kV.

Differential scanning calorimetry (d.s.c.)

D.s.c. was performed on a Perkin–Elmer DSC-II at a heating rate of 10°C min^{-1} and a range of 2 mcal s^{-1}. The sample weight was 10 to 20 mg.

Wide-angle X-ray scattering (WAXS)

WAXS studies were carried out with samples of 1 to 3 mm section thickness. Intensity was recorded as a function of scattering angle (2θ) using a General Electric diffractometer with nickel-filtered CuKα radiation.

Polarized light micrscopy

Observations were made on a Zeiss optical microscope equipped with crossed polarizers and a Mettler hot stage, employing magnifications of 20 to 160. Sections of various thicknesses were cut using a razor blade.

Molecular weight characterization

Intrinsic viscosities of the samples were measured in dimethylformamide (DMF) with glass capillaries at 30°C. Weight-average molecular weight was calculated from a relation based on light scattering data on a polyurethane of similar composition[17]:

$$[\eta] = 6.80 \times 10^{-5} M_w^{0.86}$$

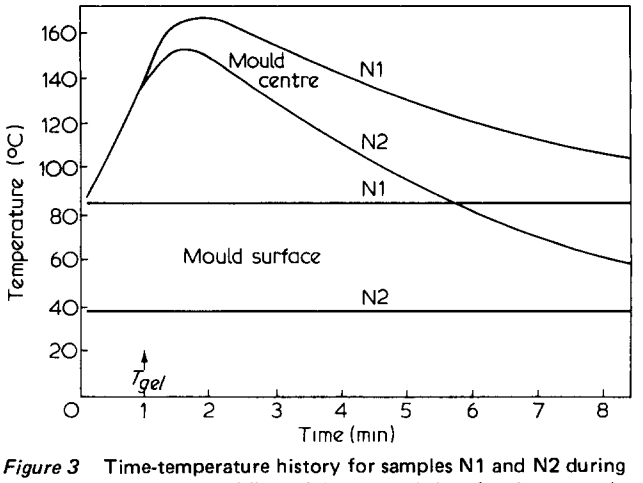

Figure 3 Time-temperature history for samples N1 and N2 during *RIM* non-isothermal moulding. Adiabatic gel time for these samples is approximately 1 min

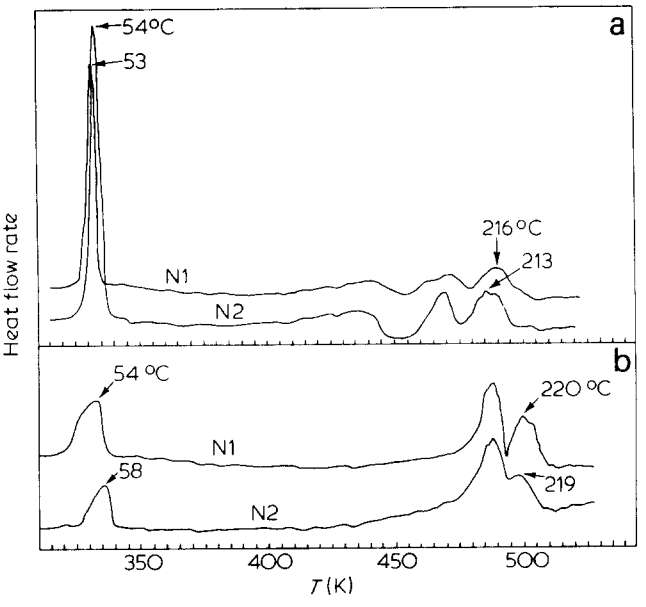

Figure 4 D.s.c. scans of samples N1 and N2. (a) Mould surface portions show sharp soft segment melting peak and broad hard segment melting peaks. (b) Mould centreline portions show increased hard segment crystallinity and diminished soft segment crystallinity

A Dupont high-pressure liquid chromatograph or g.p.c. with an ultra-violet detector was used to determine molecular weight distributions. Tetrahydrofuran was used as the solvent.

RESULTS

D.s.c.

Differential scanning calorimetry shows large differences between centreline and surface due to the temperature variations during polymerization (see *Figures 4a* and *4b*). Two clear transition regions are observed: (a) a soft segment melting endotherm at about 53° to 58°C, and (b) a hard segment melting transition at about 200° to 220°C. Only the N1-S and N2-S samples show an exotherm centred at 180°C. This exotherm for these surface samples is likely due to hard segment crystallization taking place during the d.s.c. scan. The hard segment glass transition is not observable in the Figures. T_g of the hard segment is in the range 110° to 125°C[9,12]. Seefried *et al.*[3] have calculated the theoretical T_g for totally amorphous pure PCP and report a value of −70°C. Note that the soft segment melting point and the hard segment T_g occur in the temperature range of the *RIM* process. The importance of this fact will become evident in further discussion.

The surface portions of the polymer exhibit a single soft segment melting peak at about 54°C and multiple hard segment melting peaks at approximately 195° and 215°C. Multiple hard segment endotherm peaks are consistent with the reports of other workers[7,12]. The centre portions of the polymer show a more intense hard segment domain melting between 210° and 220°C with a greatly diminished soft segment melting peak. The measured crystalline heats of fusion of both types of segments are given in *Table 1*. Comparing these values with the theoretical heat of fusion for the perfectly crystalline soft[18] and hard[19] segments we obtain relatively low degrees of crystallinity which vary from 5% (N2-C) to 14% (N2-S) for the soft segment phase and from 5% (N2-S) to 16% (N2-C) for the hard segment phase.

WAXS

A preliminary crystal structure of the pure hard segment copolymer (MDI/BDO) has recently been reported by Blackwell and Gardner[20]. The prominent *d* spacings of the MDI/BDO segment crystals are at 8.0, 4.58, 4.07 and 3.77 Å[12]. The strongest crystalline reflection is the 4.58 Å line.

No crystal structure data is available for the pure soft segment copolymer (PCP/MDI) but it is reasonable to assume that its structure is approximately that of poly(ε-caprolactone)[21] since the relatively short MDI links between the long PCP units will likely be excluded from the PCP crystals[22]. The two strongest reflections reported by Chatani *et al.*[21] for poly(ε-caprolactone) are at 4.14 and 3.74 Å. Thus, in comparing the X-ray scattering from both crystalline pure hard and pure soft segments, the 8.0 and 4.58 Å reflections are of decisive interest. A summary of the WAXS data of samples N1 and N2 is also given in *Table 1*. The WAXS scans begin at a scattering angle of 8 degrees (*d* spacing of 5.5 Å) and consequently the hard segment 8.0 Å reflection is not indicated (see *Figure 5*). The mould centre portions show three distinct crystalline reflections at 4.5, 4.1 and 3.8 Å (see *Figure 5a*). The mould surface portions show reflections only at 4.1 and 3.7 Å (see *Figure 5b*). As shown in *Figure 6*, these (soft segment) reflections disappear upon heating the sample above the soft segment melting transition.

Transmission electron microscopy

Centreline slices of both N1 and N2 samples show spherulites of fibrous texture (see *Figure 7*) similar to MDI/BDO hard segment-based spherulites as observed by Schneider[12] and Chang[22]. In the case of the N1-C sample these structures are volume filling with an average spherulite diameter of approximately 30 μm. In the case of the N2-C sample, the average spherulite diameter is about 20 μm. In addition, for the N2 samples there are occasional dense, spherical structures or 'globules', about 5 μm in diameter, at the spherulite periphery or in a featureless matrix between the spherulites.

In samples N1-S and N2-S, globular structures (diameters of 6 to 10 μm) are also observed. Their volume fraction is

Table 1 Summary of experimental data

		N1		N2	
		Centre	Surface	Centre	Surface
D.s.c. crystalline heats of fusion, (cal g^{-1})*	(soft segment)	0.8	1.2	0.7	2.1
	(hard segment)	2.5	1.7‡	2.5	0.8‡
Interplanar *d*-spacing (Å) WAXS		4.50	–	4.49	–
		4.09	4.13	4.09	4.17
		3.81	3.73	3.67	3.81
Volume fractions† ±10%	(spherulites)	0.93	0.20	0.83	0.03
	(globules)	0.04	0.35	0.12	0.53
	(matrix)	0.03	0.45	0.05	0.44
Average sizes of structures (μm), *TEM*	(spherulites)	33	35	20	20
	(globules)	8	10	4	6

* In cal g^{-1} of polymer. For pure soft segment[18] (100% crystallinity) ΔH_f = 26.4 cal g^{-1}, and for hard segment[14], ΔH_f = 35.5 cal g^{-1}

† From optical and *TEM* micrographs. Area fraction equals volume fraction for random slices through random tridimensional phases[28,29]

‡ Probably due to crystallization during d.s.c. scan

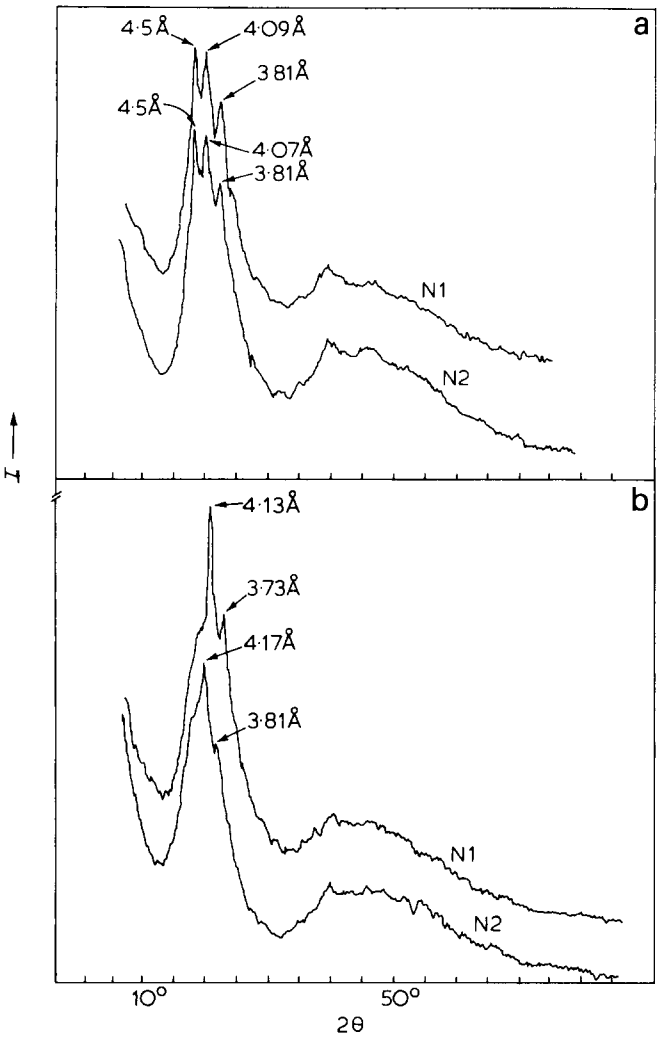

Figure 5 WAXS scans of non-isothermal *RIM* samples N1 and N2. (a) Mould centreline portions, and (b) mould surface portions

much increased while the volume fraction of hard segment spherulites is greatly diminished. The globules are again immersed in a featureless matrix. No soft segment-rich (PCP/MDI) spherulites were observed. The nature of the novel spherical structures will be discussed later.

Optical microscopy

The presence of hard segment-rich spherulites observed by *TEM* is confirmed by optical microscopy. Samples N1-C and N2-C (*Figures 8a* and *8b*) show spherulites with diffuse boundaries, normal extinction patterns (0°–90°) and negative birefringence. Samples taken from the mould surface show that the hard segment-rich spherulite volume fraction has decreased substantially for the case of N1-S and is essentially zero for N2-S. Both surface samples show the globules, previously seen by *TEM*, as weakly birefringent regions (see *Figure 9a*).

Sample N2-S exhibited large, poorly defined negatively birefringent Maltese cross patterns of about 150 μm diameter (see *Figure 9b*). The volume fractions of the different structures observed are given in *Table 1*.

Hot stage optical microscopy was performed on both samples N1-S and N2-S. The four sequential micrographs of *Figure 10* depict the effect of heating sample N1-S. Initially, there are three prominent features: (i) zones of intense birefringence; (ii) small, well-defined Maltese cross patterns; and (iii) zones of faint birefringence associated with the globules (*Figure 10a*). Near the soft segment melting point (55°C) the birefringence due to the presence of soft segment organization has vanished and consequently now both the small Maltese cross patterns and globules are better defined (*Figure 10b*). Upon further heating, the globular structures begin to coalesce at approximately 150°C, and their optical anisotropy vanishes (*Figure 10c*). After annealing for 10 min at 175°C, new hard segment-rich spherulites have nucleated in addition to the growth of existing ones (*Figure 10a*). Further heating to 220°C causes the melting of the hard segment-rich spherulites and renders the sample entirely isotropic. If the sample is heated to 175°C and held at that temperature, appreciable hard segment crystallization takes place. On cooling to room temperature, the birefringence due to soft segment organization is completely suppressed and the globules do not reappear.

Molecular weight

Intrinsic viscosity measurements were also made on these same N1 and N2 samples as well as those prepared under isothermal conditions. The results are summarized in *Table 2*. For N2, a sample taken from the surface near the cold mould wall, the molecular weight is considerably lower than at the centre of the sample. This is confirmed by the slow reacted isothermal samples. The sample reacted at 70°C has a low molecular weight.

It is also interesting to note that further heating of this sample to 150°C hardly alters its molecular weight. Once the structure is formed it is difficult to change. Only by heating to 200°C can molecular weight finally be affected, perhaps through side reactions. Similar results were found for d.s.c. measurements on these post-cured samples. Only treatment at 200°C caused a change in the d.s.c. traces.

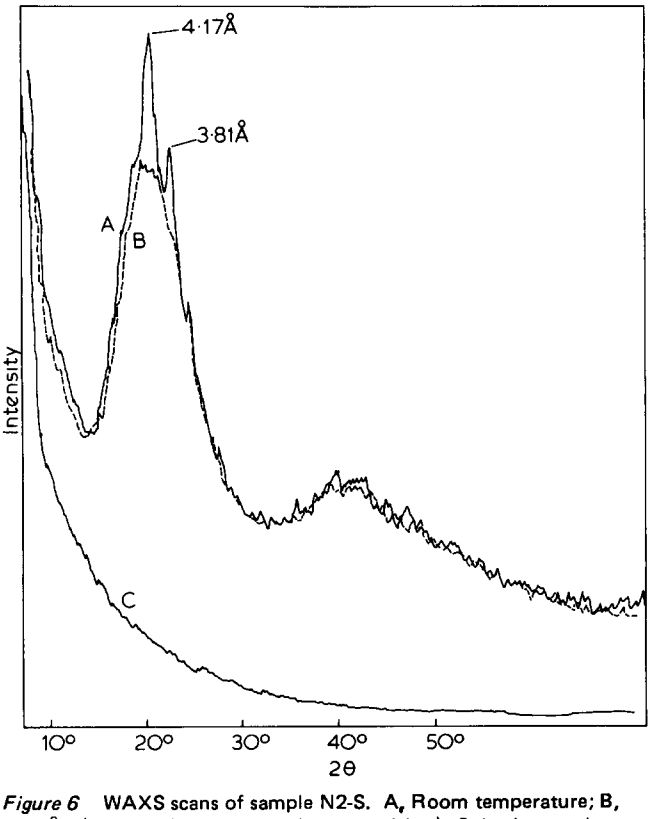

Figure 6 WAXS scans of sample N2-S. A, Room temperature; B, at 65°C (above soft segment melting transition); C, background

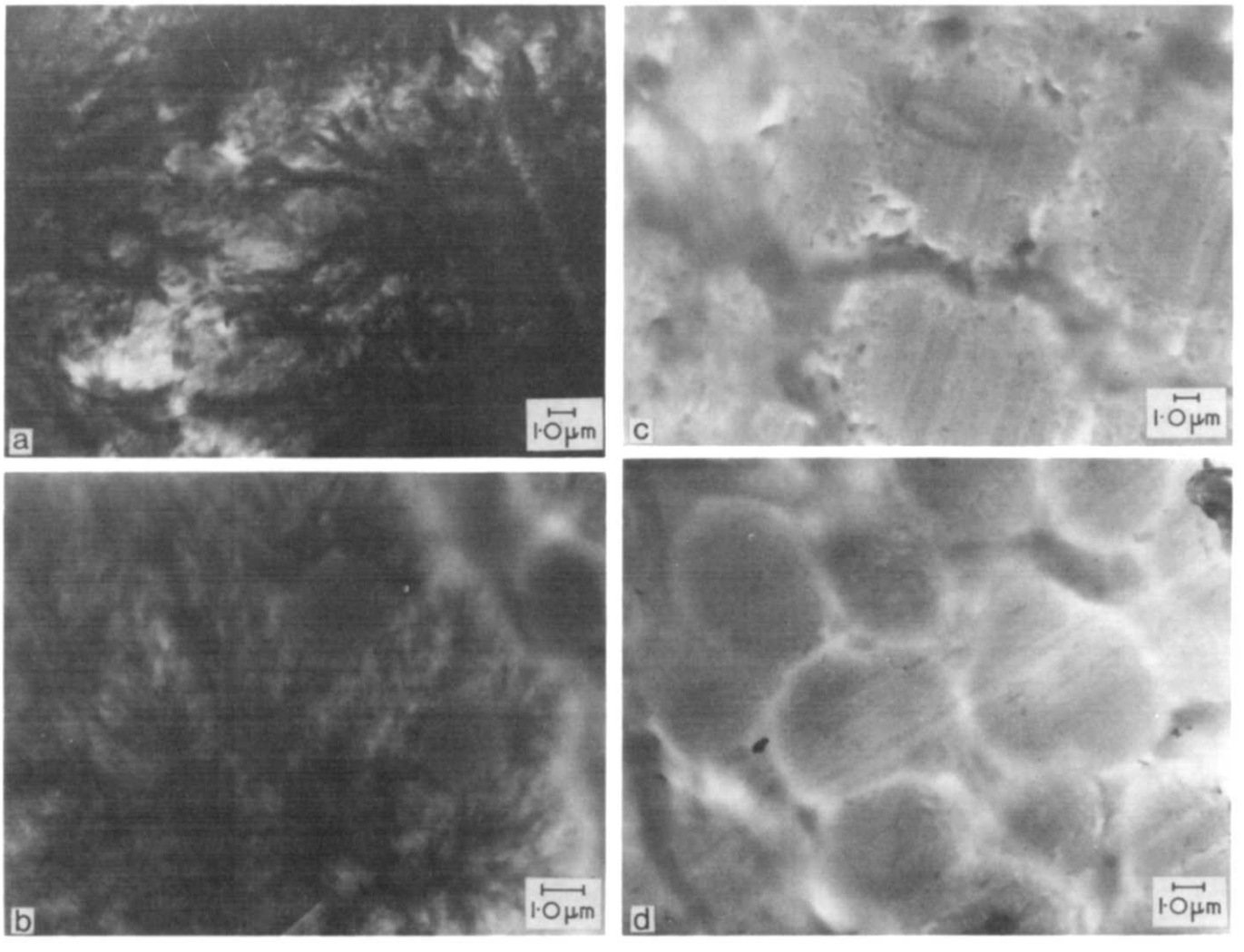

Figure 7 Bright field *TEM* micrographs of microtomed sections. (a) N1-C showing interpenetrating hard segment-rich spherulites. (b) N2-C, showing presence of globules incompatible with both hard segment-rich spherulites and soft segment-rich matrix. (c) N1-S and (d) N2-S showing densely populated globules immersed in a featureless matrix

DISCUSSION

The *RIM* samples we have examined exhibit four distinct types of morphological structures:

Hard segment crystalline domains (and spherulites)
Soft segment crystalline domains
Surface and centreline globules
Non-crystalline matrix

These structures show a strong positional dependence in the mould. Ordering of the hard segment is highest at the centre of the mould and decreases at the surface. Conversely, soft segment crystallinity is highest at the surface and decreases at the centre. Globular structures are seen to be a significant fraction of the material near the surface but diminish near the centreline. The matrix volume fraction is small at the centreline but approaches 50% at the surface.

The variation of the type of structure from surface to centreline must be attributed to the different thermal history for each location. The interdependence of the occurrence of the structures is not unexpected due to the segmented nature of the polyurethane molecules. The origin of each of the structures may be understood in terms of the temperature variation and subsequent molecular weight and segment distribution variations across the mould during the complex polymerization–phase separation–crystallization–solidification process.

The exothermic urethane reaction combined with the poor thermal conductivity of the polymer mixture will result in an approximately adiabatic temperature rise at the mould centreline; the surface region will remain approximately isothermal at the temperature set by the mould wall[16]. The peak temperature at the centreline is of the order of 100°C higher than the wall (see *Figure 3*). This centreline temperature is far above the T_m of the soft segment (55°C) but lies between the hard segment T_g and T_m (125° and 200°C). Consequently, as polymerization proceeds and the hard segment sequence length builds to a sufficient size, hard segment agglomeration and subsequent crystallization and spherulite growth occur. Because of the nature of the segmented chains, solidification (crystallization) of the longer hard segment sequences will dictate the agglomeration of those neighbouring portions of the molecules containing the soft segment (see *Figure 6* of ref 24). Non-crystallizable species (monomers, soft segment-rich molecules) must also diffuse away from the growing spherulite.

The reacting–solidifying system may be thought of as consisting of many component species: initially monomer and low molecular weight oligomers diminishing with reaction time as high molecular weight segmented polymer

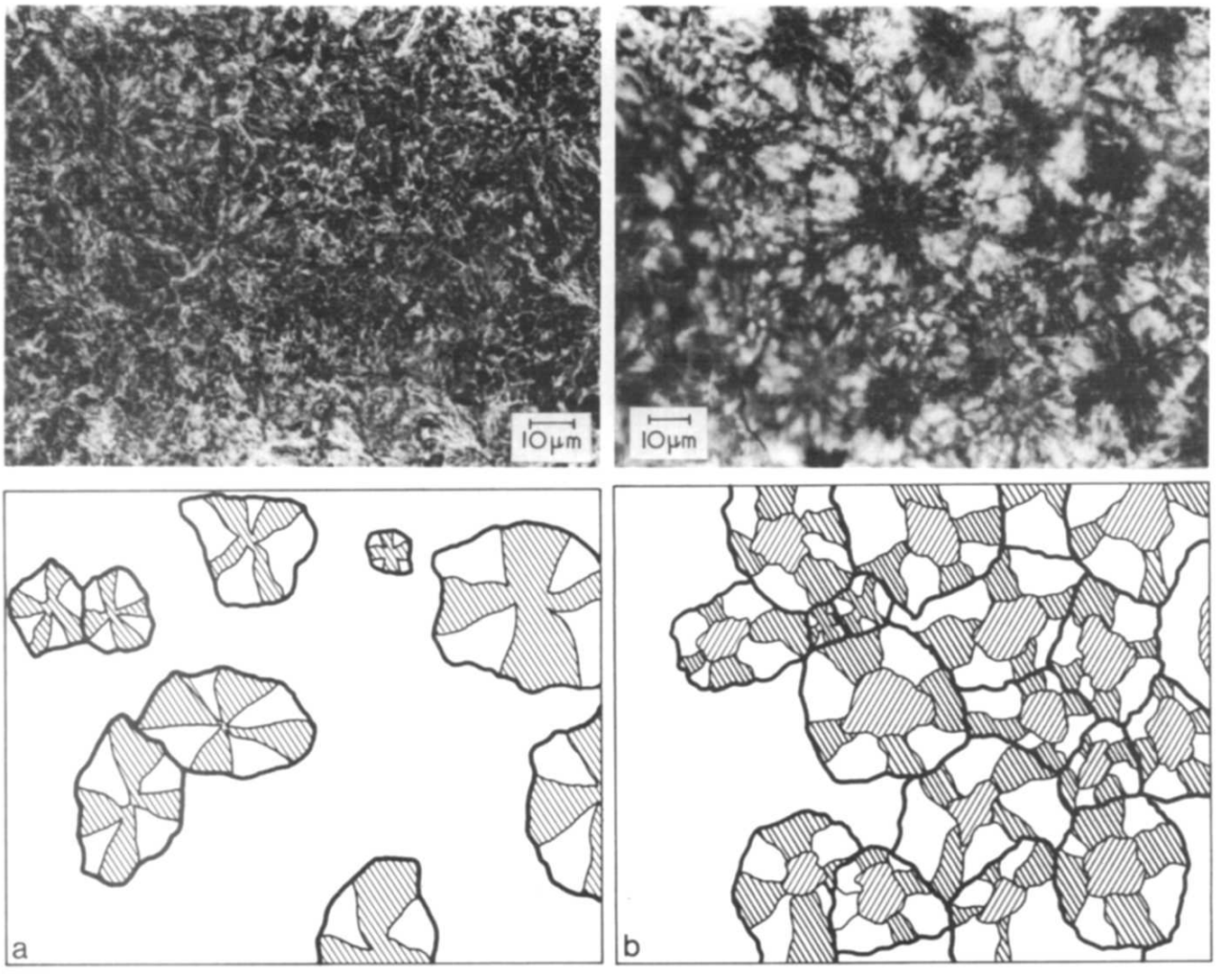

Figure 8 Optical micrographs (crossed polars) and associated schematic of structures. (a) N1-C. Note interpenetration of spherulites which complicates observation of individual entities. (b) N2-C. Note spherulites, some with non-birefringent centres

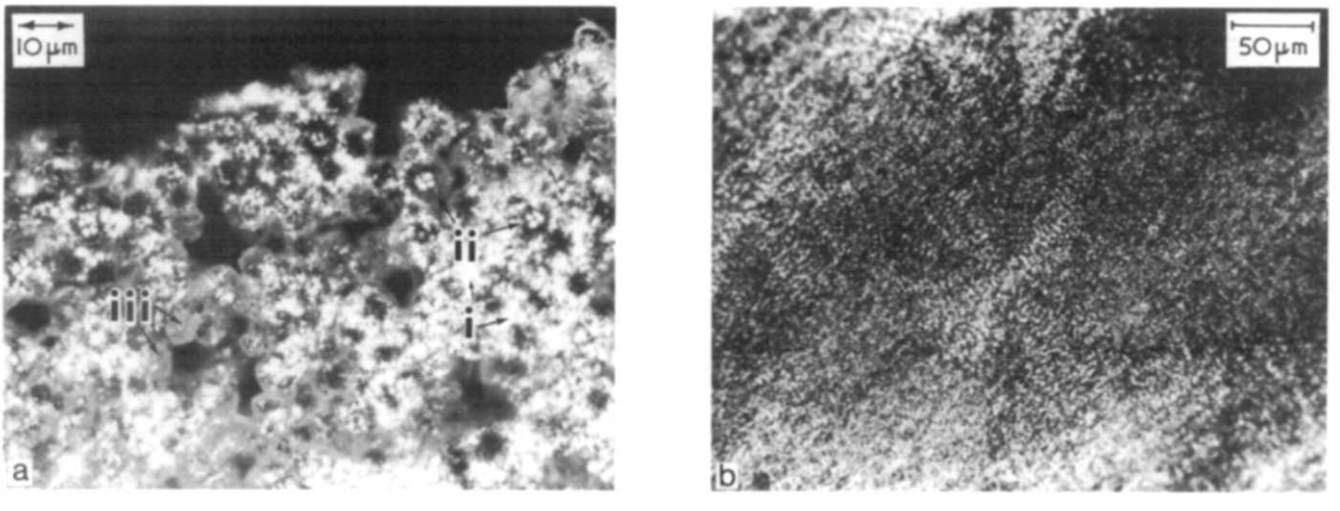

Figure 9 Optical micrographs (taken under crossed polars) of mould surface sections of *RIM* samples. (a) N1-S; (i) intense soft segment birefringence; (ii) hard segment spherulites (Maltese cross patterns); and (iii) weakly birefringent globules. (b) N2-S. Large Maltese-cross pattern which vanishes at 53°C

chains are formed. The compatibility and crystallizability of each of these species will depend on the respective sequence lengths and distributions and on the local temperature history. When the local temperature drops below the T_g of the hard segment, hard segment crystallization ceases and the mobility of the overall system becomes much less. The hard segment sequences near the surface with essentially a low isothermal history cannot aggregate and organize to form crystalline structures. However, soft segment sequences have the required temperature history for their agglomera-

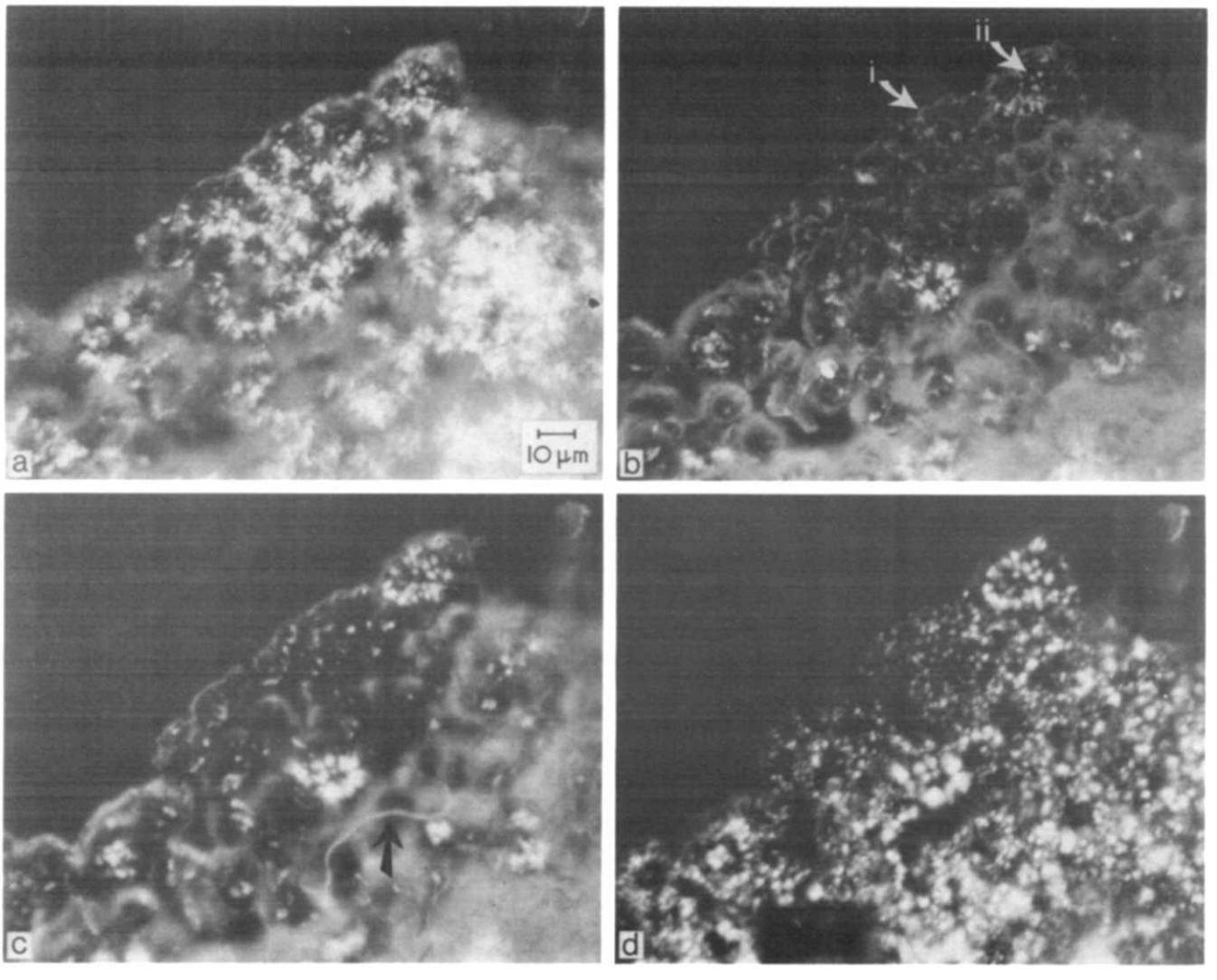

Figure 10 Heating experiment performed on N1-S sample. (a) 35°C, (b) 55°C. Soft segment organization (birefringence) has disappeared. Globules (i) and hard segment-rich spherulites (ii) are clearly discernable. (c) 150°C. Coalescence of globules is accompanied by actual sample flow (see arrow marking flow front). (d) After 10 min at 175°C. Hard segment nucleation and spherulitic growth is evident

Table 2 Molecular weight results

Sample designation		Intrinsic viscosity (DMF) $[\eta]$ (dl g^{-1})	$\bar{M}_w$
N1-C centre		0.359	21 350
N1-S surface		0.362	21 500
N2-C centre		0.477	27 500
N2-S surface		0.273	15 500
70°C	No post-cure	0.201	10 850
90°C	No post-cure	0.311	18 000
110°C	No post-cure	0.396	23 890
70°C	150°C post-cure	0.227	12 500
110°C	150°C post-cure	0.410	24 870
70°C	200°C post-cure	0.469	29 100
110°C	200°C post-cure	0.591	38 050

tion and crystallization. The soft-segment crystallinity is not as well organized as that of the hard segment–birefringent regions are visible via optical microscopy but no distinct spherulite structures based on soft-segment organization are seen. Well-developed large-scale soft segment organization is probably prevented by the hard segment-rich regions which are immobile at the lower temperatures.

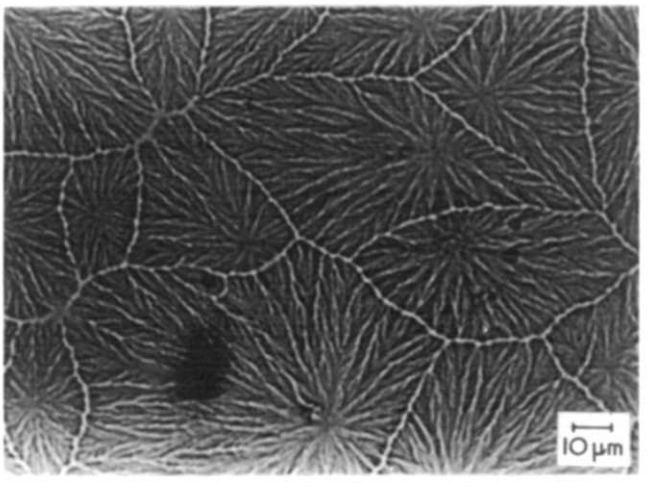

Figure 11 Optical micrograph of a DMF solution-cast N2-S sample. Note absence of surface globular structures and appearance of volume filling hard segment spherulites

In addition to the featureless matrix, spherical globules are observed both in N1 and N2 at the centreline and predominantly at the surface. At the centreline, these spherical regions are more electron dense than the surrounding matrix;

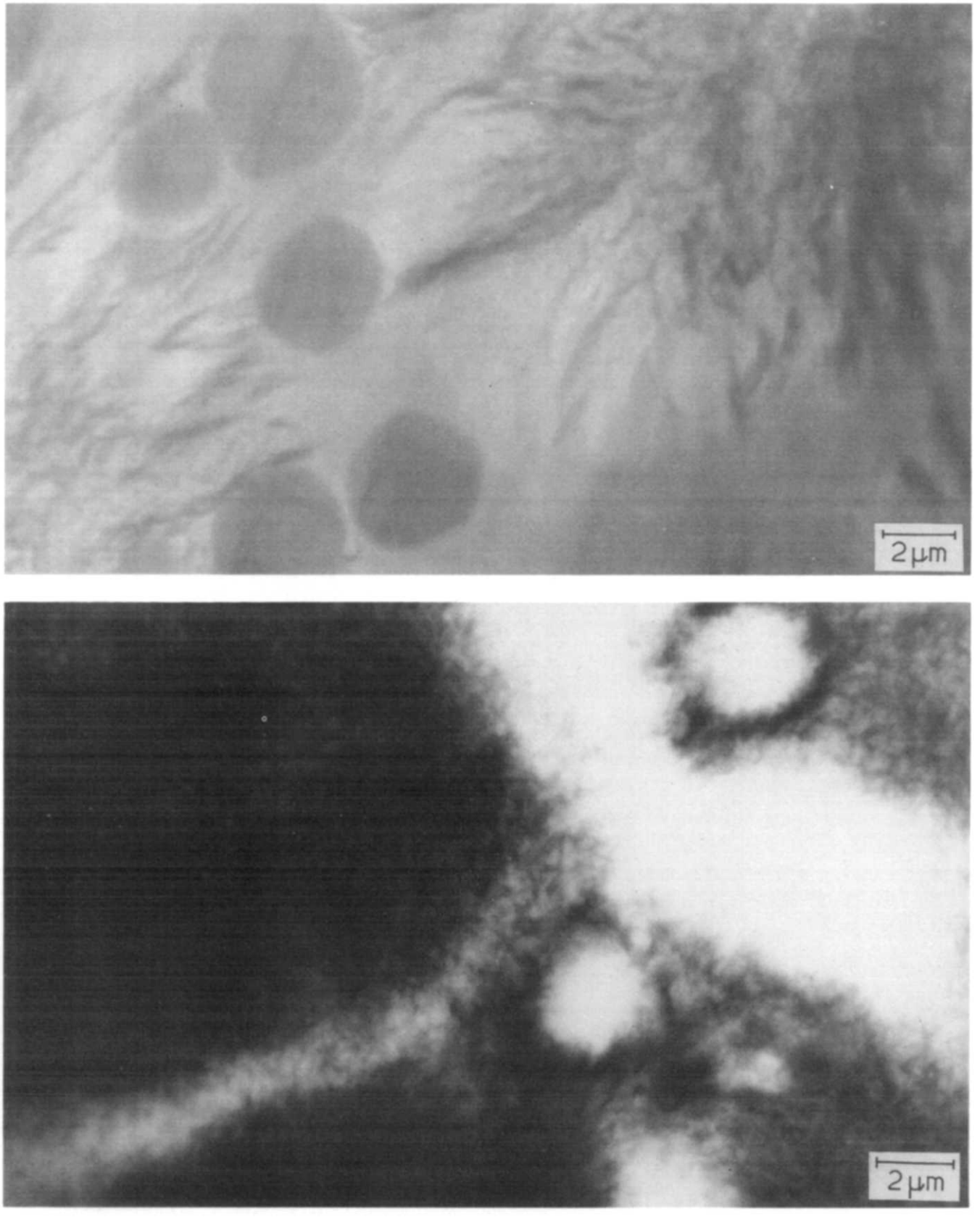

Figure 12 Hand-cast 1/6/5 PCP/MDI/BDO urethane. (a) *TEM* bright field micrograph of hand-cast sample showing hard segment with spherulites and globular structures similar to 1/6/5 PCP/MDI/BDO *RIM* sample. (b) Micrograph of hand-cast sample after annealing at 175°C for 3 h

they have featureless interiors, do not appear to coalesce mutually and appear incompatible with both the hard segment-rich spherulites and the surrounding matrix. At the surface, the globules are more volume filling and appear to be nearly equal in electron density with the matrix. A sample of N2-S containing such structures was dissolved in DMF and solution-cast from 0.5 wt % polymer in DMF at 50°C. The globules completely disappeared and only volume filling hard segment-rich spherulites are observed (see *Figure 11*). Similar surface globules have also been recently observed in

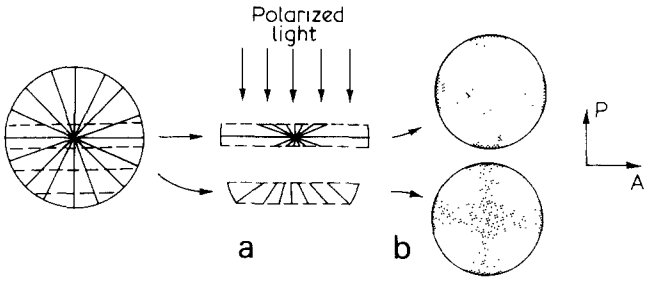

Figure 13 Schematic of spherulite microtomed slices. (a) Side view: (b) top view

a 1/5/4 PCP/MDI/BDO *RIM* system. A 1/6/5 PCP/MDI/BDO hand-cast* polymer[25] contains structures nearly identical to N2-C (see *Figure 12a*, and compare with *Figure 7b*). Elevated annealing (175°C, 3 h) of the hand cast 1/6/5 sample results in a decrease in the size of the globules with further hard segment crystallization on the globule periphery accompanied by a much decreased globule interior electron density (see *Figure 12b*).

Taken as a whole, all the data suggest that the globules consist of a mixed phase, rich in glassy hard segment. Quite possibly, the composition of the globules varies from surface to centreline. The detailed origin of these structures is not well understood at present but may be related to phase separation occurring during polymerization[23,26] and non-uniform mixing of the components[27].

The present study indicates that under *RIM* conditions where large temperature gradients exist, distinct surface and centreline microstructures develop. Two structures exist on the scale of tens of microns, the hard segment-based spherulites and the hard segment-rich glassy globules. Crystalline hard segment and soft segment domains on the scale of hundreds of Angstroms also occur. These structures are embedded in a presumably mixed non-crystalline (matrix) phase. The complex conditions of *RIM* polymerization and solidification yield matching complexity of local and large scale structures.

CONCLUSIONS

Due to the exothermic nature of urethane polymerization, mould temperature profiles and the phase separation during *RIM*, variables like molecular weight and morphology are strongly position-dependent across an *RIM* part. Morphological characteristics vary with polymerization–solidification temperatures; higher polymerization temperatures result in higher molecular weight polymer and promote better hard segment organization in the as-polymerized material. Post-curing a sample which was formed at low temperature does not improve properties to the same extent as an originally higher polymerization temperature.

For a slow *RIM* PCP/MDI/BDO urethane, a multiphased system was observed, with two scales of organization: (i) of the order of 10 μm, corresponding to hard segment spherulites and hard segment-rich glassy domains; and (ii) of the order of 100 Å, associated with hard segment spherulite fibrils and crystalline soft segment domains.

Globules, a new morphological feature, are preferentially present near the mould surface. They are proposed to be pockets of glassy hard segment-rich material which was unable to crystallize due to low temperature.

* Hand-cast here refers to polyurethane made by pouring well mixed reactants into a glass plate mould and oven reaction–curing at 145°C for 16 h

ACKNOWLEDGEMENTS

We are grateful to Dr A. K. Kulshreshtha for help with WAXS and to Mr A. L. Chang for the d.s.c. scans and hand-cast urethane annealing studies. A grant-in-aid from the Union Carbide Corporation for the support of I.D.F. and L.J.L. is gratefully acknowledged.

REFERENCES

1 Cooper, S. L. and Tobolsky, A. V. *J. Appl. Polym. Sci.* 1966, **10**, 1837
2 Critchfield, F. E., Koleske, J. V., Magnus, G. and Dodd, J. L. *J. Elastoplastics* 1972, **4**, 22
3 Seefried, C. G., Koleske, J. V., Critchfield, F. E. and Dodd, J.L. *Polym. Eng. Sci.* 1975, **15**, 646
4 Seefried, C. G., Koleske, J. V. and Critchfield, F. E. *Polym. Eng Sci.* 1976, **16**, 771
5 Huh, D. S. and Cooper, S. L. *Polymer. Eng. Sci.* 1971, **11**, 369
6 Seymour, R. W., Estes, G. M. and Cooper, S. L. *Macromolecules* 1970, **3**, 579
7 Seymour, R. W. and Cooper, S. L. *Macromolecules* 1973, **6**, 48
8 Seefried, C. G., Koleske, J. V. and Critchfield, F. E. *J. Appl. Polym. Sci.* 1975, **19**, 2493
9 Seefried, C. G., Koleske, J. V. and Critchfield, F. E. *J. Appl. Polym. Sci.* 1975, **19**, 2503
10 Allport, D. C. and Mohajer, A. A., 'Block Copolymers' (Eds. D. C. Allport and W. H. Janes) Halsted Press, NY, 1972
11 Koutsky, J. A., Hein, N. V. and Cooper, S. L. *J. Polym. Sci. (Polym. Lett.)* 1970, **8**, 353
12 Schneider, N. S., Desper, C. R., Illinger, J. L., King, A. O. and Barr, D. *J. Macromol. Sci. (B)* 1975, **11**, 527
13 Bonart, R. *J. Macromol. Sci. (B)* 1968, **2**, 115
14 Bonart, R., Morbitzer, L. and Hentze, G. *J. Macromol. Sci. (B)* 1969, **3**, 334
15 Bonart, R., Morbitzer, L. and Muller, E. H. *J. Macromol. Sci.* 1974, **9**, 447
16 Lee, L. J. and Macosko, C. W. *Soc. Plast. Eng. Tech. Papers* 1978, **24**, 151
17 Seefried, C. G., Koleske, J. V., Critchfield, F. E. and Pfaffenberg, C. R. in press
18 Crescenzi, V., Manzini, G., Calzolaroli, G. and Morry, G. *Eur. Polym. J.* 1972, **8**, 449
19 MacKnight, W. J., Yang, M. and Kajiyama, T. *Polym. Prepr.* 1968, **9**, 860
20 Blackwell, J. and Gardner, K. H. *Polymer* 1979, **20**, 13
21 Chatani, Y., Okita, Y., Tadokoro, H. and Yamashita, Y. *Polymer J.* 1970, **1**, 555
22 Chang, A. L., and Thomas, E. L. *ACS Adv. Chem. Ser.* 1979, **176**, 31
23 Tirrell, M. V., Lee, L. J. and Macosko, C. W. *ACS Symposium Series* 1979, **104**, 149
24 Fridman, I. D. and Thomas, E. L. *Polymer* 1980, **21**, 388
25 Chang, A. L., University of Massachusetts, Personal communiation
26 Nesterov, A. E., Lipatova, T. E., Dušek, K., Pelzbauer, M., Houska, M., Hradil, J. and Lipatov, Y. S. *Makromol. Chem.* 1976, **52**, 39
27 Lee, L. J., Ottino, J. M. Macosko, C. W. and Ranz, W. E. *Polym. Eng. Sci.* submitted for publication
28 Underwood, E. 'Quantitative Sereology', Addison-Wesley, Reading, Mass., 1970
29 'Proceedings of the Second International Congress for Stereology', (Ed. H. Elias) Springer–Verlag, New York, 1967, pp. 52–53

APPENDIX

Some care must be exercised in the interpretation of light optical images of microtomed samples. *Figure 8b* reveals

the appearance of hard segment-rich spherulites with non-birefringent centres of varying sizes. This is in good agreement with previous observations by Schneider *et al.*[12], and can be accounted for with the following rationale. We envision the spherulite as consisting of uniformly radiating structures (see *Figure 11*). The relative location of progressive microtomed slices with respect to the centre of the same spherulite will give rise to entirely different polarized light images. Assuming a normal birefringent spherulite, a slice containing the spherulite nucleus will display the conventional Maltese cross pattern, but as the slice is taken further away from the spherulite centre, it will be increasingly less birefringent and exhibit complete azimuthal extinction near to centre since the slice is nearly uniaxial there. The periphery of the slice will exhibit the normal Maltese cross pattern (see *Figure 11*).